

*Review Article***Chiral and Structural Analysis of Biomolecules Using Mass Spectrometry and Ion Mobility-Mass Spectrometry**JEFFREY R. ENDERS,^{1,2,3} AND JOHN A. MCLEAN^{1,2,3*}¹*Department of Chemistry, Vanderbilt University, Nashville, Tennessee*²*Vanderbilt Institute of Chemical Biology, Vanderbilt University, Nashville, Tennessee*³*Vanderbilt Institute for Integrative Biosystems Research and Education, Vanderbilt University, Nashville, Tennessee**Contribution to the special thematic project "Advances in Chiroptical Methods"*

ABSTRACT This report describes the strategies for gas-phase chiral and structural characterization of biomolecules using mass spectrometry (MS) and ion mobility-MS (IM-MS) techniques. Because both MS and IM-MS do not directly provide chiral selectivity, methodologies for adding a chiral selector are discussed in the context of (i) host–guest (H–G) associations, (ii) diastereomeric collision-induced dissociation (CID) methods, (iii) ion–molecule reactions, and (iv) the kinetic method. MS techniques for the analysis of proteins and protein complexes are briefly described. New advances in performing rapid 2D gas-phase separations on the basis of IM-MS are reviewed with a particular emphasis on the different forms of IM instrumentation and how they are used for chiral and/or structural biomolecular studies. This report is not intended to be a comprehensive review of the field, but rather to underscore the contemporary techniques that are commonly or increasingly being used to complement measurements performed by chiroptical methodologies. *Chirality* 21:E253–E264, 2009. © 2009 Wiley-Liss, Inc.

KEY WORDS: chirality; mass spectrometry; ion mobility; ion mobility-mass spectrometry; structural separations; peptide; protein

INTRODUCTION

Chiroptical techniques have found popular utility in the study of (i) chiral small molecules and (ii) large biomolecular species, such as peptides and proteins. Efficient and expedient separation and/or detection of enantiomeric pairs of small molecules are highly sought after capabilities. This is especially important for pharmaceuticals where one enantiomer of a drug may have a therapeutic effect (a eutomer) while the other may have no effect or a negative one (a distomer). Similarly, chiral properties of larger biomolecules (e.g., peptides and proteins) are used to infer information regarding secondary structural elements (e.g., α -helices, β -sheets). Many techniques have been used for chiral analyses, chief among these include electronic circular dichroism (ECD),^{1–6} vibrational circular dichroism (VCD),^{6–10} and vibrational Raman optical activity (VROA),^{11–16} each having its unique advantages and inherent challenges. One of the primary challenges of these techniques is that they can produce complex spectra, which can be difficult to interpret and may inadvertently lead to incorrect and/or biased reporting of results.^{17–20} This is especially true in the case of biomolecules that may contain electron-rich side chains (e.g., tryptophan, tyrosine) which can lead to signal interference.^{21–24}

More recently, chiral assignments have been demonstrated by using new mass spectrometry (MS) measurement strategies. Advantages of these techniques include high throughput, low limits of detection, and the potential ability to analyze chirality directly from complex mixtures. This report summarizes new avenues for gas-phase-based chiral assignments using MS, and is targeted for newer practitioners in MS techniques as well as more experienced users of MS technology interested in chiral applications. New directions in chiral analysis using 2D structural separations on the basis of ion mobility-MS (IM-MS) are presented. We review the theory and operation of typical IM-MS instrumentation and present several salient examples of using IM-MS to elucidate chirality in small molecules and structure in peptides and proteins.

Contract grant sponsor: Defense Threat Reduction Agency; Contract grant number: HDTRA1-09-1-0013

Contract grant sponsor: Vanderbilt Institute of Chemical Biology, Vanderbilt Institute for Integrative Biosystems Research and Education, Vanderbilt, University College of Arts and Sciences

*Correspondence to: John A. McLean, Department of Chemistry, Vanderbilt University, 7330 Stevenson Center, Station B 351822, Nashville, TN 37235. E-mail: john.a.mclean@vanderbilt.edu

Received for publication 30 June 2009; Accepted 9 September 2009

DOI: 10.1002/chir.20806

Published online 19 November 2009 in Wiley InterScience (www.interscience.wiley.com).

CONTEMPORARY CHIRAL AND STRUCTURAL STRATEGIES IN MASS SPECTROMETRY

Ionization Techniques in Mass Spectrometry

When performing structural analysis of chiral small molecules and/or biomolecules with MS, the two most commonly used ionization techniques are matrix-assisted laser desorption/ionization (MALDI) and electrospray ionization (ESI). Both of these ionization techniques are important to this area of research because they facilitate the generation of intact molecular ions of these species. The primary difference between MALDI and ESI is that the former allows sampling directly from solid samples, while the latter is used to ionize analytes directly from solution.

To perform MALDI, typically a weak organic acid, termed the matrix, is mixed with the analyte in large molar excess (10^3 – 10^4 :1) and allowed to cocrystallize. MALDI matrices typically exhibit three properties: (i) they contain a chromophore for the wavelength of the MALDI laser (typically in the UV range), (ii) they contain a proton-donating moiety (e.g., a carboxylic acid), and (iii) they contain an electron withdrawing group to increase the proton acidity. During MALDI irradiation, the preponderance of laser energy is deposited into the matrix molecules and little energy is deposited into the analytes of interest. Provided, when sufficient MALDI fluence is used, the matrix molecules cannot dissipate the energy over the duration of the laser pulse, resulting in the bulk ejection of material from the target including entrained analyte molecules which are subsequently ionized.²⁵

For ESI analyses, the analyte is dissolved in a solvent containing a small percentage of acid. This solution is sprayed at low flow rates (2–100 $\mu\text{l}/\text{min}$) through a fine-bore capillary that is maintained at high potential (2–4 kV). This potential causes charged species to accumulate at the tip of the capillary owing to Coulombic repulsion, forming what is termed a Taylor cone.^{26,27} Charged droplets are emitted from the Taylor cone when Coulombic forces overcome the surface tension of the solution. Thus, droplet emission can be controlled by tuning solution composition and the applied potential. As these droplets evaporate, they can result in further droplet fissioning or ejection of charged molecules. These processes continue until the analyte is completely stripped of solvent and result in gas-phase analyte ions.^{28–30}

In selecting the use of MALDI or ESI, there are three primary differences in their analytical utility. First, MALDI generally produces singly charged ions of the form $[\text{M}+\text{H}]^+$, $[\text{M}+\text{Na}]^+$, $[\text{M}+\text{K}]^+$, etc., while ESI produces singly charged ions for small molecules and typically multiply charged ions of the form $[\text{M}+n\text{H}]^{n+}$ for larger biomolecules such as peptides and proteins. In the analysis of complex mixtures, singly charged ions can result in less spectral complexity, while multiply charged ions better facilitate fragmentation studies using tandem MS strategies. Second, owing to the fundamental principles of ion generation, MALDI is more tolerant of salts than ESI, but requires empirical selection of appropriate matrices. Third, MALDI and ESI generate ions in pulsed and continuous modes, respectively. Thus the choice of MALDI or ESI

Chirality DOI 10.1002/chir

can have pragmatic implications regarding the integration of the ion source with the selected mass analyzer, but these ionization techniques are in principle complementary.

For structural analyses, it remains unclear whether the specific ion structures obtained by using MALDI or ESI are equivalent, or for biomolecules, how these structures correspond to those in the native solvated state.^{31,32} This remains an important area of ongoing research. It is likely an oversimplification to suggest that ions generated by ESI, directly from the solution phase, are able to better retain solution-phase structural elements of the analyte than those generated from the solid phase by MALDI. In both cases, at least mildly denaturing conditions are typically used in sample preparation, either by the addition of organic modifiers or acids for ESI, or by cocrystallization with small organic molecules in MALDI. Furthermore, in both cases, the anhydrous ions that are probed should ultimately adopt structures corresponding with the energy minimum attained by intramolecular folding forces, i.e., in the absence of intermolecular solvation. For both ionization techniques, it is also important to note that the internal energy imparted to the molecule from ionization can be mitigated by evaporative cooling, either from solvent evaporation in ESI or from matrix cluster evaporation in MALDI. Although challenging, future studies aimed at delineating the differences in ESI- and MALDI-derived ion structures will be highly beneficial for biophysical studies using MS-based approaches.^{33,34}

Mass Spectrometry in Chiral Analyses of Small Molecules

MS by itself is a “chirally blind” technique, because both enantiomers possess the same mass (i.e., they are isobaric). However, when used in conjunction with various chemical-based techniques, MS becomes a powerful tool for identifying and quantifying small chiral molecules. Key to each of these strategies is compliance with the Pirkle rule,^{35,36} or that of three-point intermolecular interaction, which is necessary for chiral selectivity. To create an environment conducive to Pirkle’s rule, chirally selective compounds are commonly added and interact with the enantiomers with thermodynamic selectivity. Typically, these molecules are in fact chiral molecules themselves. Choosing this chiral additive (termed a chiral selector) is usually the most difficult step for the following commonly used chiral MS techniques:

1. Host–guest (H–G) associations (Fig. 1a) center around forming diastereomeric adducts between a chiral host (chiral selector) and the enantiomeric guest (analyte). This form of analysis is performed using single-stage MS, meaning the adducts must directly differ by mass. Therefore either the host or guest compound must be isotopically labeled to allow relative chiral quantitation by ion abundance ratios. This method has been successfully implemented by a number of ionization techniques, including MALDI and ESI.^{37–43}
2. In diastereomeric collision-induced dissociation (CID) methods (Fig. 1b), diastereomeric complexes (formed

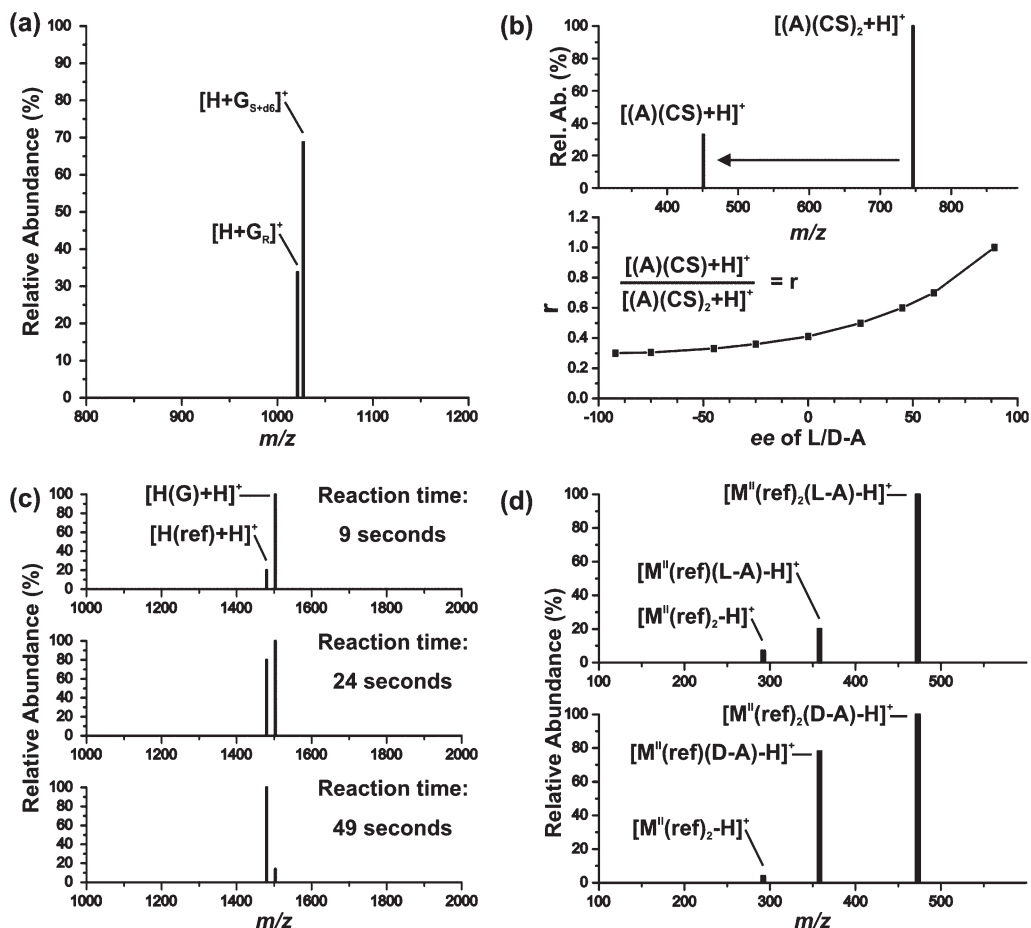


Fig. 1. Illustrative examples of the four main types of chiral analysis using mass spectrometry. (a) A hypothetical spectrum for the host-guest method, where one enantiomeric analyte guest (G_{S+de}) has been tagged with six deuterium atoms so that the enantiomers may be distinguished by single-stage mass spectrometry (Adapted from Ref. 43, with permission from Elsevier Science Ltd.). (b) Hypothetical data for the dissociative CID method. By calculating r (which is the intensity ratio of the product ion ($(A)(CS)+H^+$) to the precursor ion ($(A)(CS)_2+H^+$)), calibration curves may be plotted against the known enantiomeric excesses (ee) of the standards run. This plot is used to guide further measurement and determine the unknown ee of chiral analytes (Adapted from Ref. 46, with permission from American Chemical Society). (c) Hypothetical data for ion-molecule reactions forming a diastereomer complex $H(G)$, where the host (H) is complexed with the enantiomeric analyte molecule (G), is reacted with a reference guest molecule which replaces the enantiomeric analyte guest to produce $H(ref)$. By measuring the rates at which standards of the chiral analyte are displaced by the reference guest ($H(G) \rightarrow H(ref)$), it is possible to extract the ee of an unknown chiral mixture. For example, in this figure, if G in $H(G)$ represents the pure L form of the amino acid analyte and this $H(G)$ precursor had its intensity reduced to $\sim 20\%$ of the product ion, $H(ref)$, in 49 sec, this rate may differ from the pure D precursor form which may take 57 sec to be reduced to $\sim 20\%$ of the product ion intensity (Adapted from Ref. 48, with permission from American Chemical Society). (d) The kinetic method uses the incongruent association energies that the two forms of the enantiomer analyte possess when complexed with certain metal centers. In this figure, the two complexes, $[M^{II}(ref)_2(L-A)-H]^+$ and $[M^{II}(ref)_2(D-A)-H]^+$, fragment into $[M^{II}(ref)(D/L-A)-H]^+$ and $[M^{II}(ref)_2-H]^+$, in different proportions (Adapted from Ref. 50, with permission from American Chemical Society).

in the same fashion as H-G techniques) are fragmented using tandem MS (MS/MS). The fragmentation pattern generated is highly dependent on the interaction potentials between the chiral selector and the analyte. Because this potential energy composition is not equal for both analyte enantiomers, the fragmentation patterns for the two diastereomeric complexes will differ. Using CID negates the need for isotopic labelling, which can make this technique less expensive to implement with the proper instrumentation.⁴⁴⁻⁴⁶

- Ion-molecule reactions (Fig. 1c) involve forming diastereomeric complexes, much like the H-G and CID methods; however, subsequent to this step, these complexes are mass selected (i.e., all other masses are filtered out or removed) and are allowed to react with an

additional gas-phase reagent, which does not necessarily need to be chiral. This reaction causes displacement of both the chiral analyte and a chiral reference molecule at rates which are indicative of the chirality of the enantiomeric guest.⁴⁷⁻⁴⁹

- The kinetic method (Fig. 1d) studies the dissociation rates of cluster ions, which are typically composed of a chiral reference ligand and the chiral analyte that is attached to a metal center ($[M^{II}(ref)_2(A)-H]^+$, where M^{II} is a divalent metal, ref is either form of a chiral reference ligand, and A is either form of the chiral analyte). The chirality of the metal-bound analyte ligand affects fragmentation rates of this complex and so, based on pure chiral references of the analyte, ion abundance can lead to direct enantiomeric quantitation

in the unknown sample. This is the most commonly used form of chiral analysis involving MS. The main challenge to this approach is that it requires a relatively pure sample for analysis. This challenge, although seemingly small, makes the detection of enantiomeric molecules in complex biological samples daunting. Apart from this, a fair amount of method development must be performed on each new system that is run. Calibration curves must be generated every few days from pure enantiomers before testing, which requires that one have prior knowledge that the molecule is present in two enantiomeric forms and also that appropriate standards are available.^{50–53}

It is important to note that the predominate drawback to MS (and also spectroscopy)-based chiral techniques is that they require purified samples. This implies an inability to adequately handle concomitants and rules out the direct analysis of complex samples. Furthermore, method development for a particular system requires the derivation of complex kinetic equations to describe chiral quantification. Several excellent reviews of these techniques can be found elsewhere.^{54–56}

Mass Spectrometry for Structural Analyses of Proteins and Protein Complexes

MS has also experienced considerable utility as a structural investigation tool, providing primary structural details through CID fragmentation studies,^{57–59} and secondary and tertiary structural information through hydrogen/deuterium (H/D) exchange studies.^{60–62} Other methods such as MIKES (*mass analyzed ion kinetic energy spectrometry*), SUPREX (*stability of unpurified proteins from rates of H/D exchange*), and PLIMSTEX (*protein ligand interaction by mass spectrometry, titration, and H/D exchange*) techniques have also been described for structural analysis. These methods, however, are not typically used for chiral analysis and are outside the scope of this report. However, an excellent description of these and allied MS structural techniques can be found in a recent text by Kaltashov and Eyles.⁶³

ADVANCES IN CHIRAL AND STRUCTURAL STRATEGIES USING ION MOBILITY-MASS SPECTROMETRY

Introduction to Ion Mobility-Mass Spectrometry

Over the past decade, great strides have been made in combining rapid gas-phase biomolecular structural separations on the basis of IM with MS. The 2D separations afforded by IM-MS greatly facilitate the interpretation of complex spectra. Structural separations in IM are analogous to performing gas-phase electrophoresis in which the analytes are separated based on their size and chemical properties as they interact via collisions (10^4 – 10^6) with neutral gas molecules. In contrast with high-energy ion-neutral gas-phase collisions used in CID, IM separations use low-energy collisions to separate ions predominantly on the basis of ion-neutral collision cross section (Ω , Å²). Performing these separations in

Chirality DOI 10.1002/chir

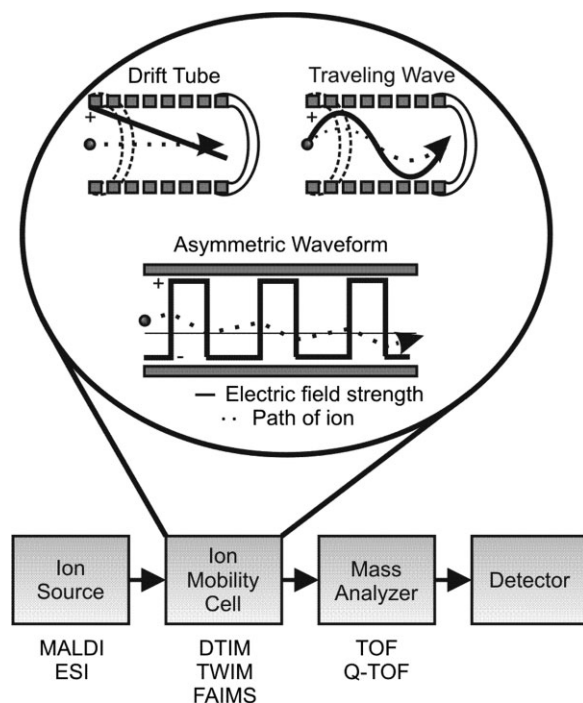


Fig. 2. A block diagram of a typical IM-MS instrument. Analytes are converted to ions in the ion source, which is typically done using MALDI or ESI. From there these ions are separated in the ion mobility cell, where the most common forms (DTIM, TWIM, and FAIMS) are illustrated in the bubble above. Space dispersive FAIMS is performed on only one mass at a time. Time-dispersive DTIM and TWIM typically use TOFMS after the ion mobility cell to analyze the entire m/z range following ion mobility separation.

the gas rather than in the condensed phase provides extremely rapid separations, 100s of microseconds to milliseconds versus minutes to hours for liquid chromatographic techniques.

Briefly, IM-mass spectrometers are composed of an ion source, an IM separation cell, a mass analyzer, and a detector as depicted in Figure 2. There are many variations to the general design, such as different ion sources (e.g., ESI and MALDI) and types of IM separation cells used, i.e., whether the ions are dispersed in time or space. The former is most commonly performed using drift tube IM (DTIM) and traveling wave IM (TWIM), while the latter is dominated by field asymmetric waveform IM (FAIMS). Although IM has been combined with virtually all of the different types of mass analyzers,⁶⁴ the most common are time-of-flight (TOF) and quadrupole-TOF (QTOF) devices. In general, following ionization, the ions are injected into a separation cell filled with a neutral drift gas and migrate under the influence of a weak electric field. The drift velocity (v_d)⁶⁵ across the drift cell is related to the electrostatic field strength (E) via the proportionality constant, which is the mobility (K) of the ion within a particular drift gas:

$$v_d = KE \quad (1)$$

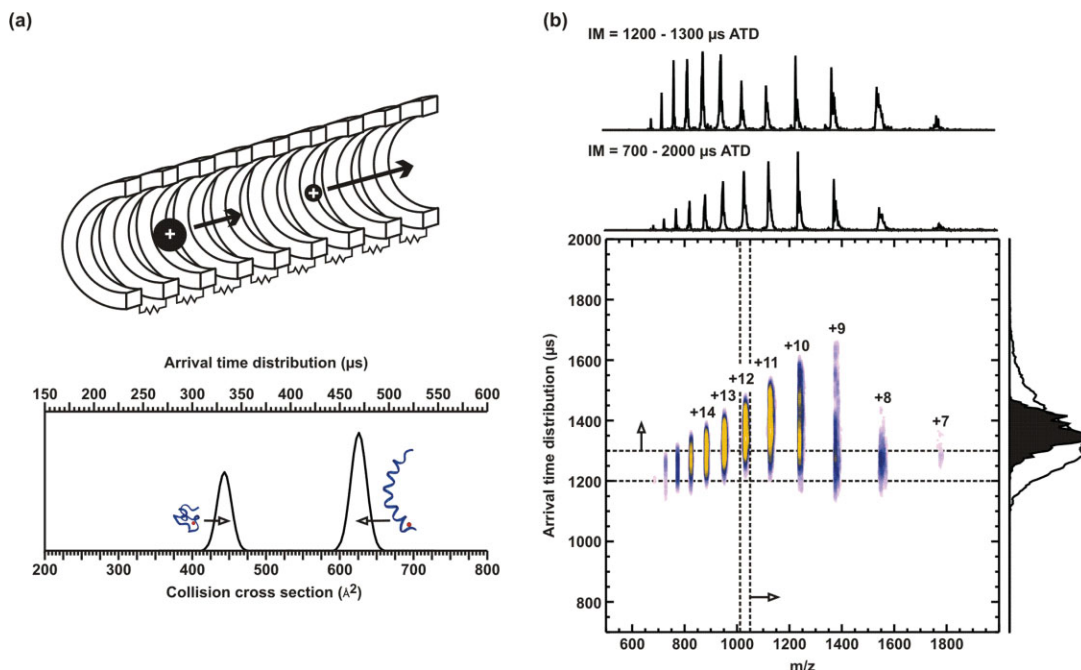


Fig. 3. (a) Depiction of the drift-tube ion mobility mode of separation. The drift tube is made up of a series of concentric rings connected in series by resistors. This creates a uniform electric field that gently guides the ions straight down the center of the drift tube in a linear path. It can be seen in the scale at the bottom that arrival time distribution is proportional to collision cross section when using this arrangement. (b) An ESI-IM-TOFMS plot of conformation space for several charge states of horse heart cytochrome c. Right: normalized IM profiles integrated over all charge states (white) and selectively for the +12 charge state (black). Top: normalized mass spectra over 700–2000 μs and selectively over 1200–1300 μs, respectively. Note the change in relative abundance for particular charge-state species upon selecting different regions of ATD (Adapted from Ref. 82, with permission from Springer Science + Business Media).

The applied electric field is electrostatic for DTIM and electrodynamic for both TWIM and FAIMS separations. It should be noted that the form of eq. 1 was specifically developed for DTIM. In the presence of the neutral drift gas, larger ions have a lower mobility than smaller ions which results in longer drift times versus shorter drift times, respectively. This effect can be thought of as a race between two skiers, one with his arms tucked at his sides and the other with his arms open wide. The skier, guided by the gradient of the hill (as ions are guided by the electric field), traveling with arms tucked will experience less drag and will reach the bottom of the hill faster.

Time Dispersive Versus Space Dispersive Ion Mobility

Ion separation in the IM cell can be accomplished by using one of the two approaches: time dispersion or space dispersion. Time-dispersive methods, such as DTIM and TWIM, separate molecular ions according to time with the higher mobility (smaller collision cross section) ions traveling through the mobility cell faster than those of lower mobility (larger collision cross section). Inherently, this method separates all ions from a sample collectively. Space-dispersive IM, namely FAIMS, uses varying electric field strengths to differentially distribute ions in space based on changes in their mobility as a function of electric-field strength. In this way, only the ions of interest are selectively directed toward the detector, while the other ions are annihilated. Hence, to collect data for multiple

analytes, the FAIMS device must be scanned using different voltages. The following sections briefly describe the different methods of IM separation, as each has unique advantages and limitations in their utility for chiral and structural analyses.

Drift Tube Ion Mobility

The DTIM design is composed of a drift tube that incorporates a series of concentric ring electrodes connected by a resistor chain (see Fig. 3) to create a uniform electric field.⁶⁶ Under the influence of this electrostatic field and in the presence of a low-molecular weight drift gas (e.g., helium, nitrogen, argon) at constant pressure, the ions separate along the axis of motion based on their mobility (i.e., the number of low-energy collisions between the ions and the drift gas molecules). Thus, ions that experience fewer collisions, because they are smaller or more structurally compact, will have shorter drift times than ions that experience a greater number of collisions, because they are larger or more structurally elongated (Fig. 3b). The inherent simplicity of the drift tube design enables the transformation of a measured drift time into absolute collision cross section by using the kinetic theory of gases.^{67–71} To a first approximation, this model assumes all the atoms in the molecules to be hard spheres and the collisions between ions and drift gas molecules to be elastic.^{72–75} Size measurements are given in terms of an orientally averaged collision cross section, which is directly proportional to the ion surface area, where the diameter of the

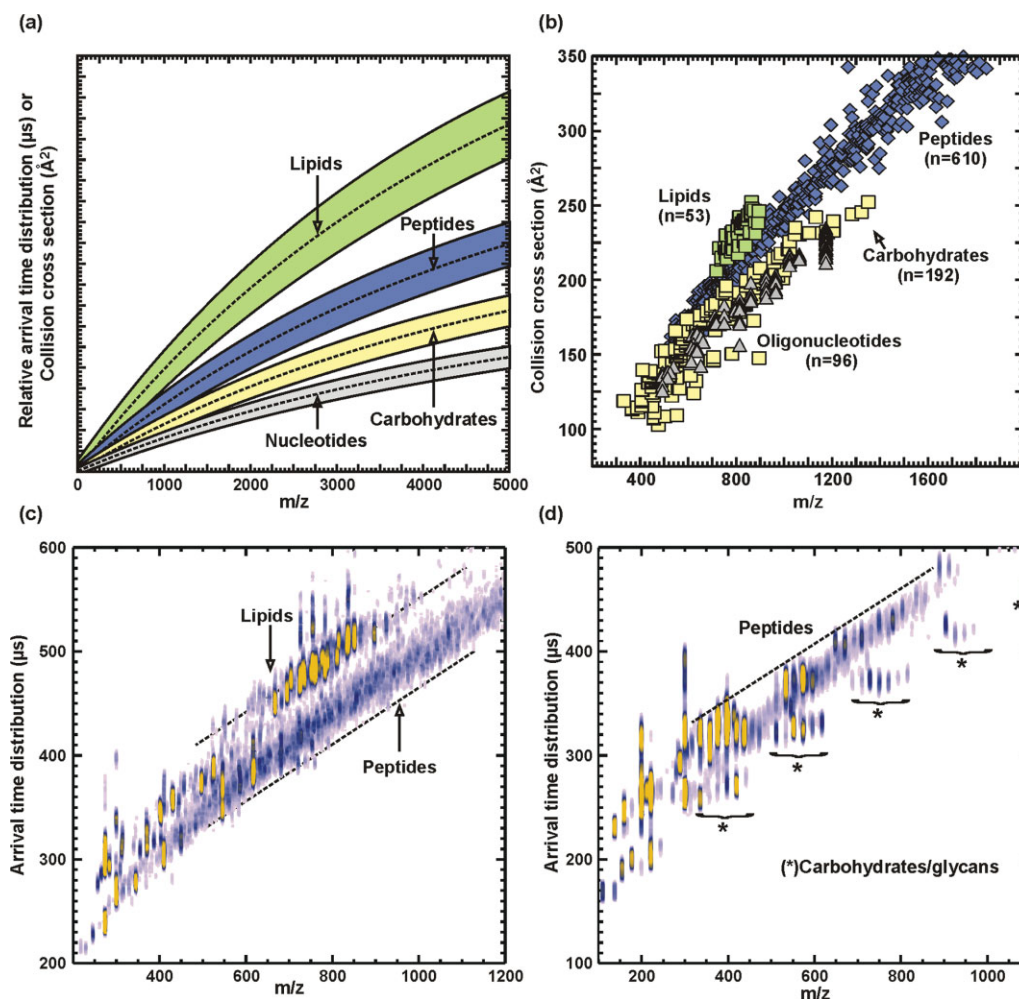


Fig. 4. A depiction of the utility of IM-MS separations for the separation of different biomolecular classes on the basis of structure. (a) A hypothetical portrayal of where singly charged analytes of different molecular class are observed in IM-MS conformation space. (b) A plot of collision cross section as a function of m/z for different biologically relevant molecular classes, including oligonucleotides, carbohydrates, peptides, and lipids. All species correspond to singly charged ions generated using MALDI. (c) A 2D plot of MALDI-IM-MS conformation space for the simultaneous analysis of lipids and peptides directly from a thin tissue section (12 μm) of a human glioblastoma. (d) A 2D plot of MALDI-IM-MS conformation space for the simultaneous analysis of peptides, glycans, and carbohydrate fragments obtained from proteolysis (trypsin) and N-linked glycan release (PNGase F) of the glycoprotein ribonuclease b. Species corresponding to carbohydrates are indicated by “*”. Dashed lines are to assist visualization of the different classes of molecules. Panels (a), (c), and (d) are adapted from Ref. 82, with permission from Springer Science+Business Media. Panel (b) is adapted from Ref. 93, with permission from Springer Science+Business Media.

sphere that describes this area is equal to the average length of the molecular ion.⁶⁷ IM resolution for DTIM typically ranges from 30 to 50 ($r = t/\Delta t$ at FWHM), whereas longer, cryogenically cooled, or higher pressure drift tubes have been reported with resolutions exceeding 100.^{76–78} Importantly, the collision cross-sectional data can be combined with molecular simulation results to interpret analyte structural and conformational detail^{31,32,79–81} (Ref. 82; Fig. 3).

Traveling Wave Ion Mobility

The commercial availability of TWIM instrumentation (Waters Corp.) has made this technology accessible to a large number of users. Similar to drift tube instruments, TWIM separates ions by time dispersion through collisions with a background drift gas, but in contrast, it uses electrodynamic fields rather than electrostatic fields.^{83,84}

Chirality DOI 10.1002/chir

This is accomplished by transmitting voltage waves sequentially across a stack of ring electrodes (Fig. 1b), which creates the so-called traveling wave.⁸⁵ Conceptually, TWIM separations are performed based on the susceptibility of different ions to the influence of the specific wave characteristics in their transmission through the mobility cell.⁷⁶ Adjustable wave parameters include traveling wave pulse height, wave velocity, and ramping either of these variables. The commercial platform (Synapt HDMS) is composed of a MALDI or ESI source, a mass resolving quadrupole, a trapping region for injecting pulses of ions into the TWIM, the TWIM drift cell, an ion transfer region, and an orthogonal TOFMS. CID can be performed in the regions before and after the TWIM drift cell. Generally resolution in the TWIM is <15 , but a new generation device reportedly provides resolutions similar to DTIM instrumentation (30–50). Nevertheless, this is sufficient for the

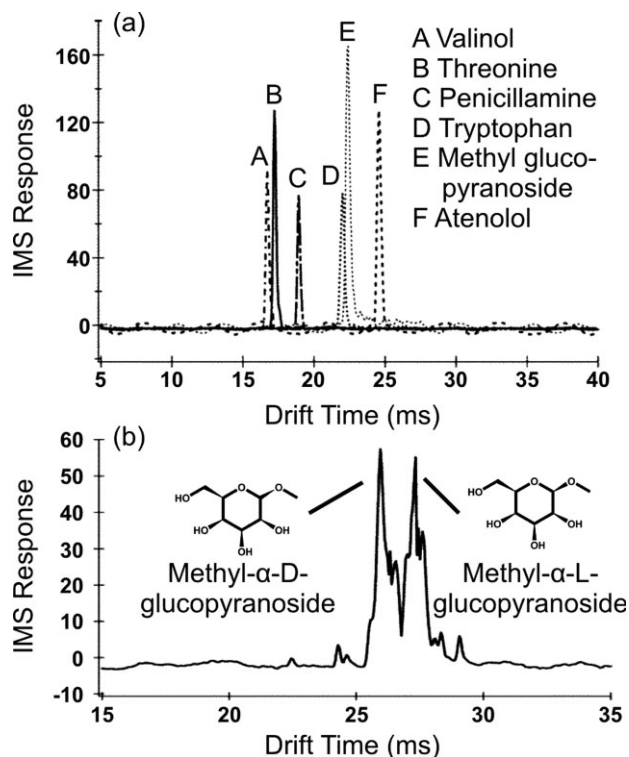


Fig. 5. (a) The mobility profile for a number of racemic mixtures of various chiral molecules separated using only nitrogen gas in the DTIM drift cell. (b) An enantiomeric separation of a racemic mixture of methyl-glucopyranoside performed by introducing 10 ppm of (S)-(+)-2-butanol into the nitrogen drift gas (Adapted from Ref. 94, with permission from American Chemical Society).

separation of molecular classes of interest (e.g., peptides from isobaric concomitant species). Although protocols have been proposed to approximate collision cross-section values using TWIM experimental data, these calculations still rely on absolute values obtained using drift tube instruments.^{86,87}

Field Asymmetric Ion Mobility

FAIMS separations were first documented in the early 1990s by Buryakov et al.^{88,89} FAIMS separations are performed on the basis of the nonlinear dependence of the mobility coefficient (K) in strongly varying electric fields. Unlike previously mentioned methods of IM separation, FAIMS performs separation in a space-dispersive manner rather than a time-dispersive manner. In FAIMS devices, ions are subjected to both positive and negative electric fields, which occur perpendicular to the direction of ion movement known as a high-frequency asymmetric waveform. By sending ions between two parallel plates in a separation cell using a longitudinal (or axial) gas flow and directing this waveform perpendicularly across them, ions that do not meet the exact criteria to traverse the cell will strike either the lower or upper plate. Only ions with particular mobility characteristics pass through the cell. The use of compensation voltage in FAIMS to achieve a mobility-based selection is roughly similar to the use of radio frequencies in quadrupole mass analyzers to achieve mass

selection. Although other IM separation methods display data as intensity versus arrival time distribution (ATD), FAIMS data are displayed as intensity versus the scanned compensation voltage.

However, one shortcoming to FAIMS is that although mass is an independent, easily calculable variable, mobility in a varying electric field is not easily predicted and depends on several variables including composition and chemical functionality, among others. Thus, it is presently not possible to make direct predictions or calculations of surface area using raw FAIMS data without first running standards and determining which compensation voltage is required for each structural representation of a particular isobaric set of ions.^{90–92}

Ion Mobility Data Interpretation

The combination of IM and MS provides a unique advantage as it provides both ion structural information by IM and mass-to-charge (m/z) information determined by accurate mass measurement by MS. Typically, IM-MS data are presented as a 3D plot with m/z on the x axis and ATD (calculated from drift velocity) on the y axis (although m/z and ATD are sometimes swapped depending on the particular instrumentation used), with false coloring used to display ion intensity (Fig. 3b). In IM-MS, the two separation dimensions exhibit a high degree of correlation, which can simultaneously be a challenge and a significant advantage. Given the relatively few types of atoms involved in the composition of most biomolecules (C, H, O, N, P, and S), the mass and volume of a molecule are largely related by a narrow range of density. This conformation space, as it is termed, has been extensively mapped for many biomolecules such as nucleotides, carbohydrates, peptides/proteins, and lipids.^{69,93} With these molecules there are inherent correlations that can be predicted for each class of analyte due to the specific structures different types of molecules preferentially adopt (Fig. 4). Although more pronounced for a m/z range over 2000, at lower ranges as that depicted in Figure 4b separations are still feasible but the correlations begin to overlap. Nevertheless, the average density for different classes of biomolecules (e.g., peptides vs. lipids) can be quite different and provides great utility in the separation of complex samples in the simultaneous measurement of different omics, e.g., lipidomics and proteomics (Fig. 4c) and glycoproteomics (Fig. 4d).

IM-MS data plotted in conformation space can be easily used to analyze multiple enantiomeric systems and/or complex samples, whereas most IM or MS techniques alone must concentrate on a single chiral analyte system. As of yet, there is not much groundwork in place for the predicted occurrence of many small molecules, including chirality, in conformation space, although there are studies in progress.^{94,95} This is due in large part to the fact that under standard conditions, enantiomers (being of similar overall size and mass) will actually overlap on this plot.

Chiral Molecule Analysis Using IM-MS

Like traditional MS, IM is in and of itself a chirally blind technique because even though chiral molecules have different orientations, they often have similar overall surface

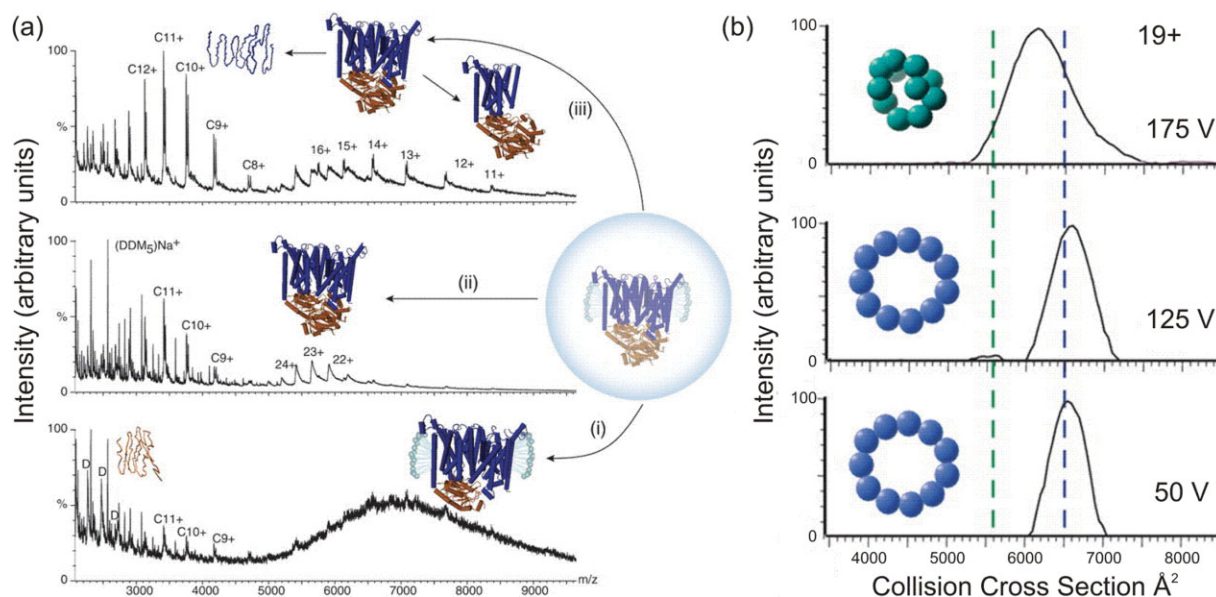


Fig. 6. (a) A depiction of the emergence of an intact membrane heteromeric protein complex (adenosine 5'-triphosphate (ATP)-binding cassette transporter, BtuC₂D₂) from a micelle contained within an electrospray droplet and the subsequent gas-phase dissociation pathways. Ions corresponding to the protein complex associated with aggregates of surfactant molecules are observed above m/z 5000. At low m/z , the dominant dissociation product is an unfolded BtuD subunit [pathway (i)]. Increasing the number of collisions results in the release of the intact tetramer [pathway (ii)]. Further increases in the number of collisions lead to the dissociation of BtuC and formation of a trimer [pathway (iii)] (Adapted from Ref. 129, with permission from American Association for the Advancement of Science). (b) Ion mobility data for the 19+ charge state of protein complex apo TRAP as a function of activation energy. The dashed lines (green and blue) represent the collision cross sections for the most collapsed structures and ring structures obtained from molecular simulations (Adapted from Ref. 130, with permission from American Association for the Advancement of Science).

areas. One approach to overcome this challenge is using a derivative of the kinetic method to complex enantiomer analytes and FAIMS to detect the subsequent intact diastereomeric complexes. This technique has been used to successfully separate many chiral molecule pairs including the enantiomers of terbutaline,⁹⁶ various amino acids,⁹⁷ D- and L-lactic acid,⁹⁸ and the diastereomers of ephedrine and pseudoephedrine.⁹⁹ The theory behind these separations cannot be handled by a trivial calculation and it is not consistently clear which structural characteristics contribute to a given complex's distinctive transmission compensation voltage (i.e., whether a more elongated structure for example requires a higher or a lower compensation voltage). Therefore, enantiopure standards need to be run to identify which components are transmitted at specific compensation voltages. Furthermore, it is not uncommon for a single enantiopure standard to produce two peaks, which can further complicate the analysis.

A 2006 study conducted by Dwivedi and coworkers took a different approach. This work involved doping the nitrogen drift gas of a DTIM instrument with a small partial pressure of chiral modifiers, (*S*)-(+)-2-butanol and (*R*)-(-)-2-butanol.⁹⁴ One enantiomer of a racemic mixture interacted with one form of the 2-butanol longer or more favorably in the separation cell and resulted in chiral selectivity (Fig. 5). Although the mechanism of this interaction was not fully modeled, it was found that by switching from (*S*)-(+)-2-butanol to (*R*)-(-)-2-butanol, the order of enantiomer elution from the drift cell was reversed. This may indicate that some form of the Pirkle rule is being satisfied in the gas phase. Using this method, separation for a num-

Chirality DOI 10.1002/chir

ber of compounds including (*R*)/(*S*)-atenolol, D/L-serine, D/L-methionine, D/L-threonine, D/L-penicillamine, D/L-valinol, D/L-phenylalanine, D/L-tryptophan, and D/L-methyl α -glucopyranoside from the respective racemic mixtures were demonstrated. All of the molecules in the study possessed only one chiral center, or few centers, and were of low molecular weight, so it is therefore unclear how larger multiple-chiral-center molecules like peptides might separate in a chiral gas-phase environment. This study by Dwivedi et al. is the only work to date that has shown IM separation on the basis of long-range interaction potentials, not purely elastic collisions, and without the need for addition of a chiral reference or complexing agent to the sample. This simplifying factor makes this technique a very promising option for the analysis of multiple chiral systems in a complex mixture.

Both the FAIMS and the buffer gas doping experiments occur via mechanisms not fully understood at this time. However, it can be concluded that with its predictability and greater ease of use that the altered bath gas method by Dwivedi has more potential to gain popularity in the near future. On a separate but similar note, separations of different forms of isomers (stereoisomers and diastereomers) have been routinely achieved in much the same way as the enantiomer separations.

Protein Structural Analysis

Apart from the small molecule systems that have been reviewed so far, protein structure analysis is another major interest in the chiral analysis community. CD and VROA are used extensively to sample the secondary structure of

various peptides and proteins. However, caution must be exercised while performing these conformational studies as CD was recently shown to give the same spectrum for a β -peptide displaying a folded and an unfolded conformation.¹⁸ Additionally, CD spectra which suffer from aromatic or sulfur-containing side-chain interferences from amino acids such as tryptophan, tyrosine, phenylalanine, cysteine, and methionine are difficult to correct although efforts in this regard have been made.¹⁰⁰

Protein analysis using IM-MS is complementary to MS in that it could not be widely used until advances in contemporary ionization techniques (i.e., MALDI¹⁰¹ and ESI¹⁰²) allowed for sampling of large biomolecules. Early IM-MS studies focused on various metallo-atomic clusters and later peptides, proteins, and other biomolecules.^{32,103–109} This work was able to demonstrate the fluidity of integration of IM into the already established MS platform.

Studies throughout the early 2000's saw IM-MS applications leading toward more intricate structural studies. For example, for systems such as nucleotide biopolymers, there is much effort being put toward trying to distinguish between 3_{10} , α -, and π -helices using chiroptical techniques.^{110–118} Counterman and Clemmer¹¹⁹ showed the ability to differentiate these motifs using IM-MS. Similarly, Jarrold and coworkers^{120–126} studied α -helices and β -sheets in unsolvated form. Julian et al.¹²⁷ performed a series of experiments to study the stability of the homochiral gas-phase serine octamer. Hill and coworkers¹²⁸ have shown the separation of isomeric peptides using standard IM conditions demonstrating that although molecular masses may be similar, overall conformation may vary to a degree that is discernable by IM-MS. In this work, separation was shown for reverse peptide sequences (i.e., Gly-Arg-Gly-Asp-Ser vs. Ser-Asp-Gly-Arg-Gly) as well as peptides differing only by two isomeric peptides (i.e., Tyr-Ala-Gly-Phe-Leu vs. Tyr-D-Ala-Gly-Phe-D-Leu) and as little as ca. 3\AA^2 difference.

Concurrent with advances in the instrumentation and ionization strategies have been the extension of IM-MS techniques for the analysis of large intact protein complexes, largely driven by Robinson and coworkers (Refs. 86, 129–131; Fig. 6) These studies use ESI-IM-MS instrumentation along with various forms of molecular dynamics to infer linkages and interaction tendencies of large heterogeneous protein complexes. Despite the fact that IM-MS protein structure analysis does not utilize the analyte's chiral characteristics per se, it gives a more complete picture of tertiary and quaternary structure. This ability extends from smaller structures (i.e., peptides, and small nucleotide oligomers) to larger structures, (i.e., proteins and intact protein complexes), which ultimately makes IM-MS a uniquely versatile tool. This technology provides a rapid means for the determination of biomolecular structure directly from complex samples, and when used in concert with appropriate chiroptical techniques, these multiple views can present a more detailed structural outlook than any one of these methods alone.¹³²

CONCLUSIONS

Gas-phase measurements of chirality and structure are increasingly being performed using MS and IM-MS measurement strategies. In MS techniques, a chiral selector is typically used to selectively interact with an enantiomer to provide quantitative information about both enantiomers present in the sample. In IM-MS measurements, chiral selectivity can be obtained through the use of a chiral selector or through using a partial pressure of chiral gas in the drift gas used for the IM separation. Furthermore, the structural information afforded by IM separations can be obtained directly from complex mixtures and from small molecules to massive protein complexes. Owing to the speed and high information content of these gas-phase measurement techniques, it is anticipated that MS and IM-MS will play an increasingly important role in chiral and structural analysis, which can complement the information derived from more traditional chiroptical techniques.

LITERATURE CITED

1. Johnson WC. Protein secondary structure and circular-dichroism—a practical guide. *Proteins: Struct Funct Genet* 1990;7:205–214.
2. Sreerama N, Woody RW. A self-consistent method for the analysis of protein secondary structure from circular dichroism. *Anal Biochem* 1993;209:32–44.
3. Woody RW. Circular-dichroism. In: Mukerji I, editor. *Biochemical spectroscopy*, Vol. 246: Methods in enzymology. San Diego: Academic Press; 1995. p 34–71.
4. McCann DM, Stephens PJ. Determination of absolute configuration using density functional theory calculations of optical rotation and electronic circular dichroism: chiral alkenes. *J Org Chem* 2006;71:6074–6098.
5. Berova N, Di Bari L, Pescitelli G. Application of electronic circular dichroism in configurational and conformational analysis of organic compounds. *Chem Soc Rev* 2007;36:914–931.
6. Stephens PJ, Pan JJ, Devlin FJ, Krohn K, Kurtan T. Determination of the absolute configurations of natural products via density functional theory calculations of vibrational circular dichroism, electronic circular dichroism, and optical rotation: the iridoids plumericin and isoplumericin. *J Org Chem* 2007;72:3521–3536.
7. Polavarapu PL, Zhao CX. Vibrational circular dichroism: a new spectroscopic tool for biomolecular structural determination. *Fresenius J Anal Chem* 2000;366:727–734.
8. Urbanova M, Setnicka V, Kral V, Volka K. Noncovalent interactions of peptides with porphyrins in aqueous solution: conformational study using vibrational CD spectroscopy. *Biopolymers* 2001;60:307–316.
9. Kuppens T, Vandyck K, Van der Eycken J, Herrebout W, van der Veken BJ, Bultinck P. Determination of the absolute configuration of three as-hydrindacene compounds by vibrational circular dichroism. *J Org Chem* 2005;70:9103–9114.
10. Stephens PJ, McCann DM, Devlin FJ, Smith AB. Determination of the absolute configurations of natural products via density functional theory calculations of optical rotation, electronic circular dichroism, and vibrational circular dichroism: the cytotoxic sesquiterpene natural products quadrone, suberosenone, suberosanone, and suberosenol A acetate. *J Nat Prod* 2006;69:1055–1064.
11. Hug W. Vibrational Raman optical-activity comes of age. *Chimia* 1994;48:386–390.
12. Barron LD, Hecht L, Bell AF, Wilson G. Recent developments in Raman optical activity of biopolymers. *Appl Spectrosc* 1996;50:619–629.
13. Barron LD, Hecht L, Blanch EW, Bell AF. Solution structure and dynamics of biomolecules from Raman optical activity. *Prog Biophys Mol Biol* 2000;73:1–49.

14. Blanch EW, Hecht L, Barron LD. Vibrational Raman optical activity of proteins, nucleic acids, and viruses. *Methods* 2003;29:196–209.
15. Barron LD, Hecht L, McColl IH, Blanch EW. Raman optical activity comes of age. *Mol Phys* 2004;102:731–744.
16. Polavarapu PL. Renaissance in chiroptical spectroscopic methods for molecular structure determination. *Chem Rec* 2007;7:125–136.
17. Tam CN, Bour P, Keiderling TA. An experimental comparison of vibrational circular dichroism and Raman optical activity with 1-amino-2-propanol and 2-amino-1-propanol as model compounds. *J Am Chem Soc* 1997;119:7061–7064.
18. Glattli A, Daura X, Seebach D, van Gunsteren WF. Can one derive the conformational preference of a beta-peptide from its CD spectrum? *J Am Chem Soc* 2002;124:12972–12978.
19. Freedberg DI, Venable RM, Rossi A, Bull TE, Pastor RW. Discriminating the helical forms of peptides by NMR and molecular dynamics simulation. *J Am Chem Soc* 2004;126:10478–10484.
20. Kelly SM, Jess TJ, Price NC. How to study proteins by circular dichroism. *Biochim Biophys Acta* 2005;1751:119–139.
21. Woody RW. Aromatic side-chain contributions to far ultraviolet circular-dichroism of peptides and proteins. *Biopolymers* 1978;17:1451–1467.
22. Woody RW. Contributions of tryptophan side chains to the far-ultraviolet circular-dichroism of proteins. *Eur Biophys J Biophys Lett* 1994;23:253–262.
23. Boren K, Freskgard PO, Carlsson U. A comparative CD study of carbonic anhydrase isoenzymes with different number of tryptophans: impact on calculation of secondary structure content. *Protein Sci* 1996;5:2479–2484.
24. Johnson WC. Analyzing protein circular dichroism spectra for accurate secondary structures. *Proteins: Struct Funct Genet* 1999;35:307–312.
25. Knochenmuss R. Ion formation mechanisms in UV-MALDI. *Analyst* 2006;131:966–986.
26. Taylor G. Disintegration of water droplets in an electric field. *Proc R Soc London Ser A* 1964;1382:383.
27. Wilm MS, Mann M. Electrospray and Taylor-cone theory, Dole's beam of macromolecules at last. *Int J Mass Spectrom Ion Processes* 1994;136:167–180.
28. Dole M, Mack LL, Hines RL. Molecular beams of macroions. *J Chem Phys* 1968;49:2240–2249.
29. Iribarne JV, Thomson BA. Evaporation of small ions from charged droplets. *J Chem Phys* 1976;64:2287–2294.
30. Fenn JB, Mann M, Meng CK, Wong SF, Whitehouse CM. Electrospray ionization—principles and practice. *Mass Spectrom Rev* 1990;9:37–70.
31. Hoaglund-Hyzer CS, Counterman AE, Clemmer DE. Anhydrous protein ions. *Chem Rev* 1999;99:3037–3079.
32. Jarrold MF. Peptides and proteins in the vapor phase. *Annu Rev Phys Chem* 2000;51:179–207.
33. Winston RL, Fitzgerald MC. Mass spectrometry as a readout of protein structure and function. *Mass Spectrom Rev* 1997;16:165–179.
34. Loo JA. Electrospray ionization mass spectrometry: a technology for studying noncovalent macromolecular complexes. *Int J Mass Spectrom* 2000;200:175–186.
35. Pirkle WH, Finn JM, Hamper BC, Schreiner J, Pribish JR. A useful and conveniently accessible chiral stationary phase for the liquid. Chromatographic separation of enantiomers. *ACS Symp Ser* 1982;185:245–260.
36. Pirkle WH, Pochapsky TC. Considerations of chiral recognition relevant to the liquid-chromatographic separation of enantiomers. *Chem Rev* 1989;89:347–362.
37. Sawada M, Okumura Y, Shizuma M, Takai Y, Hidaka Y, Yamada H, Tanaka T, Kaneda T, Hirose K, Misumi S, Takahashi S. Enantioselective complexation of carbohydrate or crown-ether hosts with organic ammonium ion guests detected by FAB mass-spectrometry. *J Am Chem Soc* 1993;115:7381–7388.
38. Chu IH, Dearden DV, Bradshaw JS, Huszthy P, Izatt RM. Chiral host-guest recognition in an ion-molecule reaction. *J Am Chem Soc* 1993;115:4318–4320.
39. Pocsfalvi G, Liptak M, Huszthy P, Bradshaw JS, Izatt RM, Vekey K. Characterization of chiral host-guest complexation in fast atom bombardment mass spectrometry. *Anal Chem* 1996;68:792–795.
40. Dobo A, Liptak M, Huszthy P, Vekey K. Chiral recognition via host-guest interactions detected by fast-atom bombardment mass spectrometry: principles and limitations. *Rapid Commun Mass Spectrom* 1997;11:889–896.
41. So MP, Wan TSM, Chan TWD. Differentiation of enantiomers using matrix-assisted laser desorption/ionization mass spectrometry. *Rapid Commun Mass Spectrom* 2000;14:692–695.
42. Schalley CA. Supramolecular chemistry goes gas phase: the mass spectrometric examination of noncovalent interactions in host-guest chemistry and molecular recognition. *Int J Mass Spectrom* 2000;194:11–39.
43. Shizuma M, Ohta M, Yamada H, Takai Y, Nakaoki T, Takeda T, Sawada M. Enantioselective complexation of chiral linear hosts containing monosaccharide moieties with chiral organic amines. *Tetrahedron* 2002;58:4319–4330.
44. Desaire H, Leary JA. Differentiation of diastereomeric *N*-acetylhexosamine monosaccharides using ion trap tandem mass spectrometry. *Anal Chem* 1999;71:1997–2002.
45. Yao ZP, Wan TSM, Kwong KP, Che CT. Chiral analysis by electrospray ionization mass spectrometry/mass spectrometry. I. Chiral recognition of 19 common amino acids. *Anal Chem* 2000;72:5383–5393.
46. Yao ZP, Wan TSM, Kwong KP, Che CT. Chiral analysis by electrospray ionization mass spectrometry/mass spectrometry. II. Determination of enantiomeric excess of amino acids. *Anal Chem* 2000;72:5394–5401.
47. Green MK, Lebrilla CB. Ion-molecule reactions as probes of gas-phase structures of peptides and proteins. *Mass Spectrom Rev* 1997;16:53–71.
48. Grigorean G, Lebrilla CB. Enantiomeric analysis of pharmaceutical compounds by ion/molecule reactions. *Anal Chem* 2001;73:1684–1691.
49. Speranza M. Enantioselectivity in gas-phase ion-molecule reactions. *Int J Mass Spectrom* 2004;232:277–317.
50. Tao WA, Zhang DX, Nikolaev EN, Cooks RG. Copper(II)-assisted enantiomeric analysis of D,L-amino acids using the kinetic method: chiral recognition and quantification in the gas phase. *J Am Chem Soc* 2000;122:10598–10609.
51. Tao WA, Gozzo FC, Cooks RG. Mass spectrometric quantitation of chiral drugs by the kinetic method. *Anal Chem* 2001;73:1692–1698.
52. Augusti DV, Carazza F, Augusti R, Tao WA, Cooks RG. Quantitative chiral analysis of sugars by electrospray ionization tandem mass spectrometry using modified amino acids as chiral reference compounds. *Anal Chem* 2002;74:3458–3462.
53. Nanita SC, Takats Z, Cooks RG. Chiral enrichment of serine via formation, dissociation, and soft landing of octameric cluster ions. *J Am Soc Mass Spectrom* 2004;15:1360–1365.
54. Tao WA, Cooks RG. Chiral analysis by MS. *Anal Chem* 2003;75:25A–31A.
55. Schug KA, Lindner W. Chiral molecular recognition for the detection and analysis of enantiomers by mass spectrometric methods. *J Sep Sci* 2005;28:1932–1955.
56. Young BL, Wu L, Cooks RG. Mass spectral methods of chiral analysis. In: Busch KW, Busch MA, editors. *Chiral analysis*. Oxford: Elsevier B. V.; 2006. p 595–659.
57. Wu QY, Vanorden S, Cheng XH, Bakhtiar R, Smith RD. Characterization of cytochrome-C variants with high-resolution FTICR mass spectrometry—correlation of fragmentation and structure. *Anal Chem* 1995;67:2498–2509.
58. Annan RS, Carr SA. The essential role of mass spectrometry in characterizing protein structure: mapping posttranslational modifications. *J Protein Chem* 1997;16:391–402.
59. Demelbauer UM, Zehl M, Plematl A, Allmaier G, Rizzi A. Determination of glycopeptide structures by multistage mass spectrometry with low-energy collision-induced dissociation: comparison of electrospray ionization quadrupole ion trap and matrix-assisted laser desorption/ionization quadrupole ion trap reflectron time-of-flight approaches. *Rapid Commun Mass Spectrom* 2004;18:1575–1582.

60. Simmons DA, Dunn SD, Konermann L. Conformational dynamics of partially denatured myoglobin studied by time-resolved electrospray mass spectrometry with online hydrogen-deuterium exchange. *Biochemistry* 2003;42:5896–5905.
61. Pan JX, Wilson DJ, Konermann L. Pulsed hydrogen exchange and electrospray charge-state distribution as complementary probes of protein structure in kinetic experiments: implications for ubiquitin folding. *Biochemistry* 2005;44:8627–8633.
62. Ferguson PL, Pan JX, Wilson DJ, Dempsey B, Lajoie G, Shilton B, Konermann L. Hydrogen/deuterium scrambling during quadrupole time-of-flight MS/MS analysis of a zinc-binding protein domain. *Anal Chem* 2007;79:153–160.
63. Kaltashov IA, Eyles SJ. *Mass spectrometry in biophysics: conformation and dynamics of biomolecules*. New York: Wiley; 2005. p282–285, 362–364.
64. Kanu AB, Dwivedi P, Tam M, Matz L, Hill HH. Ion mobility-mass spectrometry. *J Mass Spectrom* 2008;43:1–22.
65. Mason EA, McDaniel EW. Measurement of drift velocities and longitudinal diffusion coefficients. In: Mason EA, McDaniel EW, editors. *Transport properties of ions in gases*. New York: Wiley; 1988. p 31–102.
66. Mason EA, McDaniel EW. *Transport properties of ions in gases*. New York: Wiley; 1988.
67. Mack E. Average cross-sectional areas of molecules by gaseous diffusion methods. *J Am Chem Soc* 1925;47:2468–2482.
68. Dwivedi P, Wu P, Klopsch SJ, Puzon GJ, Xun L, Hill HH. Metabolic profiling by ion mobility mass spectrometry (IMMS). *Metabolomics* 2008;4:63–80.
69. Tao L, McLean JR, McLean JA, Russell DH. A collision cross-section database of singly charged peptide ions. *J Am Soc Mass Spectrom* 2007;18:1232–1238.
70. Ruotolo BT, Verbeck GF, Thomson LM, Woods AS, Gillig KJ, Russell DH. Distinguishing between phosphorylated and nonphosphorylated peptides with ion mobility-mass spectrometry. *J Proteome Res* 2002;1:303–306.
71. Furche F, Ahlrichs R, Weis P, Jacob C, Gilb S, Bierweiler T, Kappes MM. The structures of small gold cluster anions as determined by a combination of ion mobility measurements and density functional calculations. *J Chem Phys* 2002;117:6982–6990.
72. McDaniel EW. Fundamental concepts. In: McDaniel EW, editor. *Collision phenomena in ionized gases*. New York: Wiley; 1964. p 1–31.
73. Revercomb HE, Mason EA. Theory of plasma chromatography gaseous electrophoresis—review. *Anal Chem* 1975;47:970–983.
74. Shvartsburg AA, Jarrold MF. An exact hard-spheres scattering model for the mobilities of polyatomic ions. *Chem Phys Lett* 1996;261:86–91.
75. Shvartsburg AA, Schatz GC, Jarrold MF. Mobilities of carbon cluster ions: critical importance of the molecular attractive potential. *J Chem Phys* 1998;108:2416–2423.
76. Dugourd Ph, Hudgins RR, Clemmer DE, Jarrold MF. High-resolution ion mobility measurements. *Rev Sci Instrum* 1997;68:1122–1129.
77. Wyttenbach T, Kemper PR, Bowers MT. Design of a new electrospray ion mobility mass spectrometer. *Int J Mass Spectrom* 2001;212:13–23.
78. Merenbloom SI, Glaskin RS, Henson ZB, Clemmer DE. High-resolution ion cyclotron mobility spectrometry. *Anal Chem* 2009;81:1482–1487.
79. Wyttenbach T, Bowers MT. Gas-phase conformations: the ion mobility/ion chromatography method. *Mod Mass Spectrom* 2003;225:207–232.
80. McLean JA, Ruotolo BT, Gillig KJ, Russell DH. Ion mobility-mass spectrometry: a new paradigm for proteomics. *Int J Mass Spectrom* 2005;240:301–315.
81. Wyttenbach T, Bowers MT. Intermolecular interactions in biomolecular systems examined by mass spectrometry. *Annu Rev Phys Chem* 2007;58:511–533.
82. Fenn LS, McLean JA. Biomolecular structural separations by ion mobility-mass spectrometry. *Anal Bioanal Chem* 2008;391:905–909.
83. Shvartsburg AA, Smith RD. Fundamentals of traveling wave ion mobility spectrometry. *Anal Chem* 2008;80:9689–9699.
84. Giles K, Pringle SD, Worthington DL, Wildgoose JL, Bateman RH. Applications of travelling wave-based radio-frequency-only stacked ring ion guide. *Rapid Commun Mass Spectrom* 2004;18:2401–2414.
85. Pringle SD, Giles K, Wildgoose JL, Williams JP, Slade SE, Thalassinos K, Bateman RH, Bowers MT, Scrivens JH. An investigation of the mobility separation of some peptide and protein ions using a new hybrid quadrupole/travelling wave IMS/oa-ToF instrument. *Int J Mass Spectrom* 2007;261:1–12.
86. Ruotolo BT, Benesch JLP, Sandercock AM, Hyung S-J, Robinson CV. Ion mobility-mass spectrometry analysis of large protein complexes. *Nat Protoc* 2008;3:1139–1152.
87. Williams JP, Scrivens JH. Coupling desorption electrospray ionization and neutral desorption/extractive electrospray ionization with a travelling-wave based ion mobility mass spectrometer for the analysis of drugs. *Rapid Commun Mass Spectrom* 2008;22:187–196.
88. Buryakov IA, Krylov EV, Makas AL, Nazarov EG, Pervukhin VV, Rasulev UK. Ion division by their mobility in high tension altering electric field. *Pisma V Zhurnal Tekhnicheskoi Fiziki* 1991;17:60–65.
89. Buryakov IA, Krylov EV, Nazarov EG, Rasulev UK. A new method of separation of multi-atomic ions by mobility at atmospheric-pressure using a high-frequency amplitude-asymmetric strong electric-field. *Int J Mass Spectrom Ion Processes* 1993;128:143–148.
90. Krylov EV, Nazarov EG, Miller RA. Differential mobility spectrometer: model of operation. *Int J Mass Spectrom* 2007;266:76–85.
91. Shvartsburg AA, Tang K, Smith RD. Optimization of the design and operation of FAIMS analyzers. *J Am Soc Mass Spectrom* 2005;16:2–12.
92. Shvartsburg AA, Bryskiewicz T, Purves RW, Tang KQ, Guevremont R, Smith RD. Field asymmetric waveform ion mobility spectrometry studies of proteins: dipole alignment in ion mobility spectrometry? *J Phys Chem B* 2006;110:21966–21980.
93. Fenn LS, Kliman M, Mahsut A, Zhao SR, McLean JA. Characterizing ion mobility-mass spectrometry conformation space for the analysis of complex biological samples. *Anal Bioanal Chem* 2009;394:235–244.
94. Dwivedi P, Wu C, Matz LM, Clowers BH, Siems WF, Hill HH. Gas-phase chiral separations by ion mobility spectrometry. *Anal Chem* 2006;78:8200–8206.
95. McLean JA. The mass-mobility correlation redux: the conformational landscape of anhydrous biomolecules. *J Am Soc Mass Spectrom* 2009; 20:1775–1781.
96. Mie A, Ray A, Axelsson BO, Jornten-Karlsson M, Reimann CT. Terbutaline enantiomer separation and quantification by complexation and field asymmetric ion mobility spectrometry-tandem mass spectrometry. *Anal Chem* 2008;80:4133–4140.
97. Mie A, Jornten-Karlsson M, Axelsson BO, Ray A, Reimann CT. Enantiomer separation of amino acids by complexation with chiral reference compounds and high-field asymmetric waveform ion mobility spectrometry: preliminary results and possible limitations. *Anal Chem* 2007;79:2850–2858.
98. Sultan J, Gabryelski W. Structural identification of highly polar nontarget contaminants in drinking water by ESI-FAIMS-Q-TOF-MS. *Anal Chem* 2006;78:2905–2917.
99. McCooeye M, Ding L, Gardner GJ, Fraser CA, Lam J, Sturgeon RE, Mester Z. Separation and quantitation of the stereoisomers of ephedra alkaloids in natural health products using flow injection-electrospray ionization-high field asymmetric waveform ion mobility spectrometry-mass spectrometry. *Anal Chem* 2003;75:2538–2542.
100. Krittanai C, Johnson WC. Correcting the circular dichroism spectra of peptides for contributions of absorbing side chains. *Anal Biochem* 1997;253:57–64.
101. Fenn JB, Mann M, Meng CK, Wong SF, Whitehouse CM. Electrospray ionization for mass-spectrometry of large biomolecules. *Science* 1989;246:64–71.
102. Karas M, Hillenkamp F. Laser desorption ionization of proteins with molecular masses exceeding 1000 daltons. *Anal Chem* 1988;60:2299–2301.
103. St Louis RH, Hill HH. Ion mobility spectrometry in analytical chemistry. *Crit Rev Anal Chem* 1990;21:321–355.

104. Hill HH, Siems WF, Stlouis RH, McMinn DG. Ion mobility spectrometry. *Anal Chem* 1990;62:A1201–A1209.
105. Eiceman GA. Advances in ion mobility spectrometry—1980–1990. *Crit Rev Anal Chem* 1991;22:17–36.
106. Wyttenbach T, vonHelden G, Bowers MT. Gas-phase conformation of biological molecules: bradykinin. *J Am Chem Soc* 1996;118:8355–8364.
107. Clemmer DE, Jarrold MF. Ion mobility measurements and their applications to clusters and biomolecules. *J Mass Spectrom* 1997;32:577–592.
108. Hoaglund CS, Valentine SJ, Sporleder CR, Reilly JP, Clemmer DE. Three-dimensional ion mobility TOFMS analysis of electrosprayed biomolecules. *Anal Chem* 1998;70:2236–2242.
109. Jarrold MF. Unfolding, refolding, and hydration of proteins in the gas phase. *Acc Chem Res* 1999;32:360–367.
110. Sudha TS, Vijayakumar EKS, Balaran P. Circular-dichroism studies of helical oligopeptides—can 310 and α -helical conformations be chirally distinguished. *Int J Pept Protein Res* 1983;22:464–468.
111. Yasui SC, Keiderling TA, Bonora GM, Toniolo C. Vibrational circular dichroism of polypeptides. V. A study of 3(10)-helical-octapeptides. *Biopolymers* 1986;25:79–89.
112. Yasui SC, Keiderling TA, Formaggio F, Bonora GM, Toniolo C. Vibrational circular dichroism of polypeptides. IX. A study of chain-length dependence for 3(10)-helix formation in solution. *J Am Chem Soc* 1986;108:4988–4993.
113. Toniolo C, Polese A, Formaggio F, Crisma M, Kamphuis J. Circular dichroism spectrum of a peptide 3(10)-helix. *J Am Chem Soc* 1996;118:2744–2745.
114. Andersen NH, Liu ZH, Prickett KS. Efforts toward deriving the CD spectrum of a 3(10) helix in aqueous medium. *FEBS Lett* 1996;399:47–52.
115. Yokum TS, Gauthier TJ, Hammer RP, McLaughlin ML. Solvent effects on the 3(10)-/alpha-helix equilibrium in short amphipathic peptides rich in α, α -disubstituted amino acids. *J Am Chem Soc* 1997;119:1167–1168.
116. Wallimann P, Kennedy RJ, Kemp DS. Large circular dichroism ellipticities for N-templated helical polypeptides are inconsistent with currently accepted helicity algorithms. *Angew Chem Int Ed Engl* 1999;38:1290–1292.
117. Silva R, Yasui SC, Kubelka J, Formaggio F, Crisma M, Toniolo C, Keiderling TA. Discriminating 3(10)- from α helices: vibrational and electronic CD and IR absorption study of related Aib-containing oligopeptides. *Biopolymers* 2002;65:229–243.
118. Armen R, Alonso DOV, Daggett V. The role of α -, 3(10)-, and π -helix in helix \rightarrow coil transitions. *Protein Sci* 2003;12:1145–1157.
119. Counterman AE, Clemmer DE. Gas phase polyaniline: assessment of $i \rightarrow i+3$ and $i \rightarrow i+4$ helical turns in [Ala(*n*) +4H](4+) (*n* = 29–49) ion. *J Phys Chem B* 2002;106:12045–12051.
120. Kaleta DT, Jarrold MF. Helix-turn-helix motifs in unsolvated peptides. *J Am Chem Soc* 2003;125:7186–7187.
121. Breaux GA, Jarrold MF. Probing helix formation in unsolvated peptides. *J Am Chem Soc* 2003;125:10740–10747.
122. Kohtani M, Jones TC, Schneider JE, Jarrold MF. Extreme stability of an unsolvated alpha-helix. *J Am Chem Soc* 2004;126:7420–7421.
123. Sudha R, Kohtani M, Jarrold MF. Non-covalent interactions between unsolvated peptides: helical complexes based on acid–base interactions. *J Phys Chem B* 2005;109:6442–6447.
124. Dugourd P, Antoine R, Breaux G, Broyer M, Jarrold MF. Entropic stabilization of isolated beta-sheets. *J Am Chem Soc* 2005;127:4675–4679.
125. Sudha R, Jarrold MF. Left-handed and ambidextrous helices in the gas phase. *J Phys Chem B* 2005;109:11777–11780.
126. Jarrold MF. Helices and sheets in vacuo. *Phys Chem Chem Phys* 2007;9:1659–1671.
127. Julian RR, Hodyss R, Kinnear B, Jarrold MF, Beauchamp JL. Nanocrystalline aggregation of serine detected by electrospray ionization mass spectrometry: origin of the stable homochiral gas-phase serine octamer. *J Phys Chem B* 2002;106:1219–1228.
128. Wu C, Siems WF, Klasmeier J, Hill HH. Separation of isomeric peptides using electrospray ionization/high-resolution ion mobility spectrometry. *Anal Chem* 2000;72:391–395.
129. Barrera NP, Di Bartolo N, Booth PJ, Robinson CV. Micelles protect membrane complexes from solution to vacuum. *Science* 2008;321:243–246.
130. Ruotolo BT, Giles K, Campuzano I, Sandercock AM, Bateman RH, Robinson CV. Evidence for macromolecular protein rings in the absence of bulk water. *Science* 2005;310:1658–1661.
131. Benesch JLP. Collisional activation of protein complexes: picking up the pieces. *J Am Soc Mass Spectrom* 2009;20:341–348.
132. Ruotolo BT, Russell DH. Gas-phase conformations of proteolytically derived protein fragments: influence of solvent on peptide conformation. *J Phys Chem B* 2004;108:15321–15331.